ADVANCED ENERGY MATERIALS
www.advenergymat.de

# Impact of Triplet Excited States on the Open-Circuit Voltage of Organic Solar Cells

*Johannes Benduhn,* Fortunato Piersimoni, Giacomo Londi, Anton Kirch, Johannes Widmer, Christian Koerner, David Beljonne, Dieter Neher, Donato Spoltore, and Koen Vandewal**

**The best organic solar cells (OSCs) achieve comparable peak external quantum efficiencies and fill factors as conventional photovoltaic devices. However, their voltage losses are much higher, in particular those due to nonradiative recombination. To investigate the possible role of triplet states on the donor or acceptor materials in this process, model systems comprising Zn- and Cu-phthalocyanine (Pc), as well as fluorinated versions of these donors, combined with $C_{60}$ as acceptor are studied. Fluorination allows tuning the energy level alignment between the lowest energy triplet state ($T_1$) and the charge-transfer (CT) state, while the replacement of Zn by Cu as the central metal in the Pcs leads to a largely enhanced spin–orbit coupling. Only in the latter case, a substantial influence of the triplet state on the nonradiative voltage losses is observed. In contrast, it is found that for a large series of typical OSC materials, the relative energy level alignment between $T_1$ and the CT state does not substantially affect nonradiative voltage losses.**

In contrast to organic light emitting diodes (OLEDs), organic solar cells (OSCs) are still awaiting a market breakthrough.[1–3] A major challenge for OSCs is their relatively low power conversion efficiency (PCE).[4,5] The main reason is their low open-circuit voltage ($V_{OC}$) as compared to the optical gap ($E_{opt}$) of the main absorbing materials.[6]

All photovoltaic (PV) technologies suffer from voltage losses, arising from fundamental radiative recombination and parasitic nonradiative recombination. Radiative recombination is inevitable, and is the only recombination process taking place in an ideal solar cell.[7–10] This process determines the upper limit of the $V_{OC}$, denoted as the radiative open-circuit voltage $V_r$. In reality, the measured $V_{OC}$ is lower than $V_r$ due to the presence of nonradiative decay channels, lowering $V_r$ by $\Delta V_{nr}$

$$\Delta V_{nr} = V_r - V_{OC} \tag{1}$$

Rau has shown that $\Delta V_{nr}$ is proportional to the natural logarithm of the quantum efficiency of emission ($EQE_{EL}$).[7] The validity of Equation (1) for OSCs has been shown previously,[11,12] where $\Delta V_{nr}$ typically accounts for 0.25–0.40 V of the total voltage losses ($\Delta V_{OC} = E_{CT} - V_{OC}$).[8,12–14] This is a much higher value than in inorganic and Perovskite solar cells, where $\Delta V_{nr} \leq 0.15$ V.[15–17]

In addition to voltage losses due to radiative and nonradiative recombination, OSCs suffer voltage losses because the photogenerated excitons on the donor (D) or acceptor (A) undergo a charge transfer to form an interfacial charge-transfer (CT) state with energy $E_{CT}$. However, it has been recently shown that the energy difference between the optical gap of the donor or acceptor and the CT state ($E_{opt} - E_{CT}$) can be minimized to less than 0.05 eV[13,18] and even down to 0.01 eV,[6] without sacrificing efficient free charge carrier generation. Therefore, in the OSCs with the currently lowest voltage losses, nonradiative recombination is the main reason for the low $V_{OC}$ as compared to other PV technologies employing absorber with similar optical gaps.

In a previous study, we have shown for a whole range of solution and vacuum processed OSCs that $\Delta V_{nr}$ correlates with $E_{CT}$. This led us to the conclusion that nonradiative decay is mediated by CT state decay via electron–phonon coupling.[12] However, in the related OLED technology, the major nonradiative decay channel is mediated by the triplet excited states.[19] In OSCs, triplet states are present on both the D and A materials, and for high voltage OSCs the energy of the lowest energy

J. Benduhn, A. Kirch, Dr. J. Widmer,[+] Dr. C. Koerner,[++] Dr. D. Spoltore, Prof. K. Vandewal[+++]
Dresden Integrated Center for Applied Physics and Photonic Materials (IAPP) and Institute for Applied Physics
Technische Universität Dresden
Nöthnitzer Str. 61, 01187 Dresden, Germany
E-mail: johannes.benduhn@iapp.de; koen.vandewal@uhasselt.be
Dr. F. Piersimoni, Prof. D. Neher
Institute of Physics and Astronomy
University of Potsdam
Karl-Liebknecht-Str. 24–25, 14476 Potsdam, Germany
G. Londi, Prof. D. Beljonne
Chimie des Matériaux Nouveaux & Centre d'Innovation et de Recherche en Matériaux Polymères
Université de Mons
Place du Parc 20, 7000 Mons, Belgium
The ORCID identification number(s) for the author(s) of this article can be found under https://doi.org/10.1002/aenm.201800451.
[+]Present address: Heliatek GmbH, Treidlerstraße 3, 01139 Dresden, Germany
[++]Present address: Organic Electronics Saxony, Würzburger Str. 51, 01187 Dresden, Germany
[+++]Present address: Institute for Materials Research (IMO-IMOMEC), Hasselt University, Wetenschapspark 1, 3590 Diepenbeek, Belgium

DOI: 10.1002/aenm.201800451

 

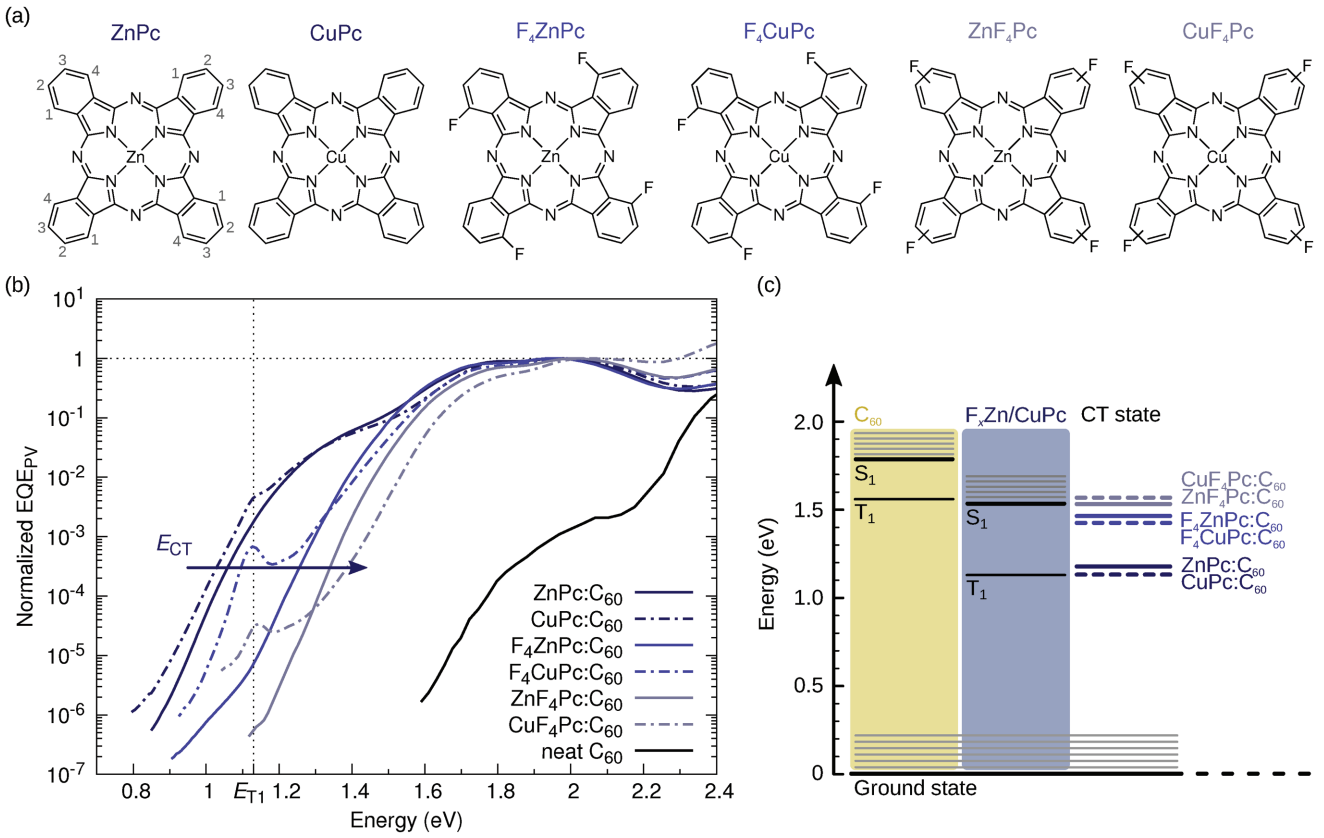


**Figure 1.** a) Molecular structures of the donor molecules and their short names used throughout the manuscript. In the molecular structure of ZnPc, the free bonding positions at the benzene ring are numbered. For the donors $ZnF_4Pc$ and $CuF_4Pc$, fluorine binds either to position (2) or (3) of the corresponding benzene ring. b) Normalized sensitive $EQE_{PV}$ spectra as a function of the photonenergy for OSCs comprising the above shown donor molecules and $C_{60}$ as acceptor. The ZnPc series is shown with solid blue lines. The CuPc series, represented by dash-dot blue lines, shows distinct photocurrent feature at 1.13 eV, related to triplet absorption. c) Shows the corresponding energy levels of the pure absorbers and the corresponding CT state.

triplet state $T_1$ ($E_{T1}$) on one or both compounds may be lower than $E_{CT}$.[20–22] Moreover, Chow et al. reported that recombination via $T_1$ can drive a large fraction of the overall recombination in OSCs.[23]

In this paper, we therefore investigate under which circumstances, low energy $T_1$ states affect nonradiative recombination losses and the $V_{OC}$ of OSCs. We study model systems comprising Zn- and Cu-phthalocyanines (ZnPc, CuPc) combined with $C_{60}$ as electron acceptor. Fluorination of the phthalocyanines (Pcs) results in an increase of the CT state energy, lifting it 0.33–0.40 eV above the $T_1$ state of the donor. Surprisingly, we find that, in contrast to OLEDs, $T_1$ is not the main responsible for the dominating nonradiative decay in typical OSCs. We generalize this finding by studying a substantial amount of OSCs. Only in the case of a large coupling of $T_1$ to the ground state, introduced for example by the presence of Cu, nonradiative decay via $T_1$ significantly contributes to the voltage losses.

To investigate the impact of $T_1$ on $\Delta V_{nr}$, we chose suitable model systems comprising the donors ZnPc, CuPc, and their fluorinated derivatives. See **Figure 1**a for the molecular structures. These donors are coevaporated with $C_{60}$ as acceptor and used as absorber in OSCs. Fluorination increases $E_{CT}$, while the minimum singlet ($S_1$) excitation energy $E_{S1}$ remains relatively invariant. Employing Cu as a central metal atom is an elegant way to precisely obtain $E_{T1}$. Indeed, optical transitions from and to the triplet manifold of Pcs containing Cu are possible due to the fact that Cu has an unpaired $4s^1$ electron in the standard electron configuration, mediating a spin flip.[24,25] When comparing OSCs employing $C_{60}$ as acceptor and either ZnPc or CuPc as donor molecules, we notice for CuPc indeed an additional absorption feature at 1.13 eV, see Figure 1b.[26] This additional absorption appears at the same position in OSCs with fluorinated derivatives of CuPc. Moreover, we find for these OSCs electroluminescence (EL) peaks at similar photon energies, see Figures S2 and S3 in the Supporting Information. This additional absorption and emission is not visible in any of the ZnPc-based devices and has been directly linked to the enhanced coupling of $T_1$ to the ground state in CuPc, mediated by the unpaired $4s^1$ electron.[24–27] Therefore, we obtain $E_{T1}$ = 1.13 eV from the crossing point of reduced $EQE_{PV}$ and EL spectra of $F_4CuPc$ and $CuF_4Pc$, see Figure S3 in the Supporting Information. Since the wavefunction of $T_1$ of metal–Pc is mainly located on the organic ligand, the Pc, we expect that the $E_{T1}$ values for ZnPc and its fluorinations are very similar to $E_{T1}$ of the CuPc compounds. In order to shed some light on the nature of the low-energy electronic transitions and assess their

energies and oscillator strengths, we performed highly correlated complete active space self-consistent field (CASSCF) calculations. These indicate that $E_{S1}$ and $E_{T1}$ vary only weakly with chemical structure across the series of compounds investigated (see Table S4 in the Supporting Information). Most importantly, the calculated oscillator strength of $T_1$ for Cu-based Pc's is 150–800 fold higher than that of the Zn-based molecules. More details of the calculations can be found in the Supporting Information. Results from Vincett and co-workers confirm the value of $E_{T1}$ which we obtained, by directly observing phosphorescence of CuPc and ZnPc in solution at 77 K, with a peak energy of 1.16 and 1.13 eV, respectively.[27] Moreover, thin films of CuPc, measured at room temperature, showed photoluminescence at a peak position of $E$ = 1.12–1.13 eV, further confirming the obtained $E_{T1}$ in our thin films.[28–30]

When fluorinating ZnPc or CuPc, the energy of the highest occupied molecular orbital (HOMO) and the lowest unoccupied molecular orbital (LUMO) shifts away from the vacuum level simultaneously,[31] resulting in a similar $E_{S1}$ for all donor molecules, see Figure S1a in the Supporting Information. In the first type of fluorination ($F_4$–metal–Pc), all four fluorine atoms are attached only to equivalent positions (1) or (4) of the outer benzene ring. In the second case, denoted metal–$F_4$Pc, the four fluorine atoms can be attached randomly either to position (2) or (3) of the benzene ring, which is schematically sketched in Figure 1a. All these configurations of metal–$F_4$Pc are chemically and energetically very similar and not distinguishable.

$E_{CT}$ of the OSCs is obtained from sensitive $EQE_{PV}$ and EL spectra as outlined earlier.[8] The values of $E_{CT}$ are listed in **Table 1**, more details on the determination procedure can be found in Figure S2 in the Supporting Information. As shown in Figure 1b,c, fluorination leads to shifted positions of the HOMO and LUMO of the donor molecules, resulting in an increased $E_{CT}$. While $T_1$ is clearly the lowest energy state for the fluorinated Pcs, $V_{OC}$ still correlates with $E_{CT}$ rather than $E_{T1}$, for both the Zn- and Cu- containing blends. We discuss this in more detail in the next paragraphs.

The bar diagram in **Figure 2** summarizes the energetic situation and voltage losses for the six different OSCs. The height of each bar depicts $E_{CT}$ of the corresponding device. The $V_{OC}$ is reduced as compared to $E_{CT}$ due to fundamental radiative voltage losses ($\Delta V_r$, shown in light green), and parasitic nonradiative voltage losses ($\Delta V_{nr}$, shown in yellow). Radiative

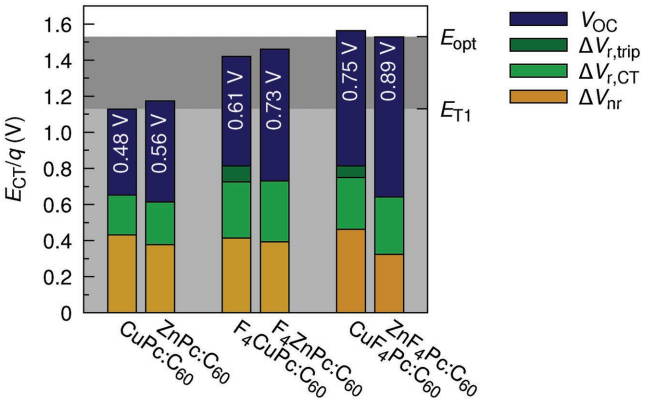


**Figure 2.** Detailed representation of the voltage losses in the series of OSCs consisting of the metal–Pc donor series and $C_{60}$ as acceptor. The dark grey area represents $E_{opt}$ of the donor and the light grey area highlights the donor's $E_{T1}$. The height of the full column represents $E_{CT}$, divided by the elementary charge $q$. The dark blue column represents the measured $V_{OC}$. The green bar represents the fundamental radiative voltage losses, and the yellow bar the nonradiative voltage losses, which were obtained by taking the difference between the calculated $V_r$ and the measured $V_{OC}$. For the OSCs comprising $F_4$CuPc and Cu$F_4$Pc, the increased coupling of the triplet–doublet to the ground state causes additional voltage losses due to radiative triplet state decay, shown as a dark green bar.

and nonradiative voltage losses are calculated from the sensitively measured $EQE_{PV}$ and EL spectra, following the method outlined in ref. [8]. Additional $\Delta V_r$ caused by radiative decay of $T_1$ are obtained from the difference between the $V_r$ values calculated with and without considering the absorption of $T_1$ (highlighted in dark green). The optical gap ($E_{opt}$) of the device corresponds to the $E_{S1}$ of the donor, being at ≈1.53 eV, since it is lower than that of $C_{60}$.

Within each of the three pairs of donor molecules containing either Zn or Cu (nonfluorinated and two differently fluorinated metal–Pc's) $E_{CT}$ is very comparable. However, $V_{OC}$ is always significantly lower for devices containing Cu as compared to Zn. The $E_{CT}$ of CuPc:$C_{60}$ is about 0.04 eV smaller than that of ZnPc:$C_{60}$, but the $V_{OC}$ for CuPc:$C_{60}$ is about 0.08 V lower because $\Delta V_{nr}$ is increased by 0.05 V and $\Delta V_r$ is slightly decreased. When fluorinating CuPc to $F_4$CuPc, $E_{CT}$ increases and, as compared to CuPc, the voltage losses $E_{CT}/q - V_{OC}$

**Table 1.** Information on the OSC performance of the metal–Pc:$C_{60}$ series.

| Donor | $j_{SC}$[a)] [mA cm$^{-2}$] | FF[d)] [%] | PCE[d)] [%] | $V_{OC}$[d)] [V] | $V_r$[b)] [V] | $E_{CT}$[c)] [eV] | $V_0$[d)] [V] | $E_{CT} - qV_0$ [eV] |
|---|---|---|---|---|---|---|---|---|
| ZnPc | 8.1 | 59.4 | 2.7 | 0.56 | 0.94 | 1.17 | 1.10 ± 0.02 | 0.07 ± 0.02 |
| CuPc | 6.9 | 49.0 | 1.6 | 0.48 | 0.91 | 1.13 | 1.05 ± 0.01 | 0.08 ± 0.01 |
| $F_4$ZnPc | 7.3 | 58.1 | 3.1 | 0.73 | 1.12 | 1.46* | 1.31 ± 0.02 | 0.15 ± 0.02 |
| $F_4$CuPc | 2.4 | 41.0 | 0.6 | 0.61 | 1.02 | 1.42* | 1.17 ± 0.01 | 0.25 ± 0.01 |
| Zn$F_4$Pc | 2.2 | 33.1 | 0.6 | 0.89 | 1.21 | 1.53* | 1.43 ± 0.02 | 0.10 ± 0.02 |
| Cu$F_4$Pc | 0.5 | 29.4 | 0.1 | 0.75 | 1.21 | 1.56* | 1.48 ± 0.01 | 0.08 ± 0.01 |

[a)]The listed performance values correspond to a mismatch corrected illumination with simulated sunlight at an intensity of 1000 Wm$^{-2}$; [b)]$V_r$ was calculated from the $EQE_{PV}$ and EL spectra, assuming the reciprocity relation between absorption and emission;[7,8] [c)]$E_{CT}$ was obtained from Gaussian fit to the $EQE_{PV}$ and EL spectra following ref. [8]. If denoted with *, $E_{CT}$ was obtained from the crossing point between $EQE_{PV}$ and EL, for more information see Figure S2 in the Supporting Information; [d)]$V_0$ represents the $V_{OC}$ extrapolated to 0 K and was obtained from temperature dependent $j$–$V$ curves at different illumination intensities. The denoted $V_0$ represents the mean value for seven different illumination intensities and the statistical error of the mean value.

increase drastically. Here, $T_1$ is the lowest energy level in the system and due to the substantial oscillator strength of the $T_1$-to-ground-state transition, the total radiative recombination increases and consequently reduces the $V_{OC}$. The radiative character of the additional recombination, introduced by $T_1$, in the $F_4CuPc:C_{60}$ device can be seen in the EL spectra in Figure S2 in the Supporting Information. In $CuPc:C_{60}$ the radiative recombination is instead mediated by the CT state. Indeed, for the $F_4ZnPc$ device, voltage losses $E_{CT}/q - V_{OC}$ are 0.08 V smaller as compared to $F_4CuPc$, which can be fully attributed to the absence of radiative losses through $T_1$. In the OSCs containing $ZnF_4Pc$ and $CuF_4Pc$, the voltage losses for the $CuF_4Pc$-based device are even more pronounced and $\Delta V_{nr}$ and $\Delta V_r$ are both significantly higher as compared to $ZnF_4Pc$.

When comparing the overall performance of the OSCs, it is immediately clear that, although the films absorb a similar amount of light (see Figure S1b in the Supporting Information), the $j_{SC}$ and FF for Cu containing OSCs are always lower than for the Zn containing ones, especially when $E_{T1} < E_{CT}$ (case of $F_4CuPc$ and $CuF_4Pc$). This indicates an increased coupling of $T_1$ in the Cu containing compounds, harmful for charge generation and extraction. However, details of the charge generation and extraction processes in this series of compounds are beyond the scope of this paper.

To understand the possible impacts of $T_1$ on the voltage losses in more detail, we analyzed basic recombination rate equations, c.f. Figure S5 in the Supporting Information. In the case that $E_{T1}$ is lower than $E_{CT}$, we deduce three important cases

(i) When $T_1$ states repopulate the CT state faster than decaying but its decay rate is higher than direct CT state decay, all excited states are in equilibrium and in the limit of $T \to 0$ K, $V_{OC}$ approaches $E_{T1}$.
(ii) When $T_1$ decays faster or similarly fast than $T_1$ dissociation into CT states, then $T_1$ states are not in equilibrium with CT states and free carriers, causing extra recombination losses via $T_1$ population and decay. In the limit of $T \to 0$ K, $V_{OC}$ approaches $E_{CT}$.
(iii) When recombination via the CT state is faster than the population and decay of $T_1$, the impact of $T_1$ is negligible. In the limit of $T \to 0$ K, $V_{OC}$ approaches $E_{CT}$.

Temperature dependent $j$–$V$ curves performed at different light intensities allow us to determine which particular case applies to a certain device. From extrapolation of $V_{OC}$ to $T \to 0$ K, $V_0$ is obtained and compared to $E_{T1}$ and $E_{CT}$. The experimental data is shown in Figure S4 in the Supporting Information and the values are listed in Table 1 for each device. For all OSCs where the splitting between $T_1$ and $E_{CT}$ is relatively small (ZnPc, CuPc) and for the donors $F_4ZnPc$ and $ZnF_4Pc$, we find $V_0 \approx E_{CT}$, with $V_0$ being slightly (≈0.10 eV) lower than $E_{CT}$. This indicates that even if $T_1$ is the lowest energy state, it does not affect $V_0$ when the coupling of $T_1$ to ground state is indeed small (case (ii) or (iii)). The slightly lower $V_0$ than $E_{CT}$ is due to the fact that $E_{CT}$ slightly decreases upon cooling as reported in ref. [8,32]. However, for $F_4CuPc$, we observe $V_0 \approx E_{T1}$, located 0.25 eV below $E_{CT}$. This indicates that $T_1$, the CT state, and the free charge carriers are in equilibrium and that the recombination to the ground state is mediated by $T_1$ (case (i)). For $CuF_4Pc$, we find that $V_0 \approx E_{CT} \approx E_{opt}$. Here, recombination involves the $S_1$ state in this OSC and $V_0$ corresponds to $E_{opt}$. For this configuration $T_1$ just adds recombination losses for $T > 0$ K (case (ii)).

In summary, we find that if $T_1$ is lower than $E_{CT}$ and if its coupling to the ground state is high, e.g., the case of $F_4CuPc$, it significantly increases the total voltage losses $\Delta V_{OC}$ (case (i)) as compared to the normal case, where the $T_1$-ground-state coupling is much weaker (e.g., $F_4ZnPc$). Only in the latter case $V_{OC}$ is expected to correlate with $E_{CT}$ independently from the exact position of the lower laying $T_1$. However, it is still unclear if in this case, $T_1$ causes additional $\Delta V_{nr}$. Therefore, we investigate $\Delta V_{nr}$ for a series of archetypical OSC materials including cases where $E_{T1}$ is higher and lower than $E_{CT}$.

For commonly used OSC materials the determination of $E_{T1}$ is difficult due to the fact that optical transitions between $T_1$ and the ground state are forbidden. In the literature, several alternative approaches have been reported to obtain $E_{T1}$. Local $T_1$ states always have a lower energy than $S_1$ because of the exchange energy of the antibonding spin state, which is usually assumed not be larger than 1 eV.[19,33–36] One method to obtain $E_{T1}$ is to circumvent the low electronic coupling of $T_1$ to the ground state by substituting heavy atoms and thereby enhancing the phosphorescence. $E_{T1}$ is then assumed to be similar in energy as for the original molecule.[19] Another indirect way is to use a host–guest system, in which the quenching of the emission of a series of guest molecules can provide an estimation of the relative energetic position of $T_1$.[19,36] Alternatively, density functional theory calculations have been used to predict $E_{T1}$, but uncertainties of the absolute value are often rather large.

In **Figure 3**, we compare $\Delta V_{nr}$ for a large set of OSCs, distinguishing different relative alignments of $T_1$ and the CT state. The $\Delta V_{nr}$ values were partly published in ref. [12] and

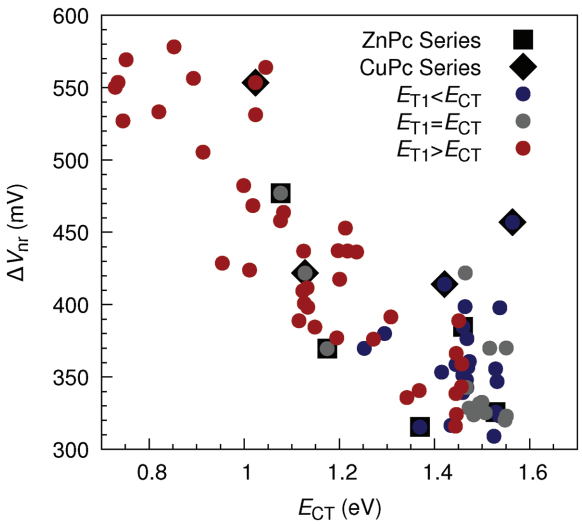


**Figure 3.** Comparison of $\Delta V_{nr}$ for several OSCs with either $E_{T1} > E_{CT}$ or $E_{T1} < E_{CT}$ indicated by red or blue filled circles, respectively. Since determination of $E_{T1}$ is difficult, grey filled circles represent OSCs where published values present an uncertainty of $E_{T1} - E_{CT} \leq \pm 100$ meV. The black squares and diamonds indicate the investigated series of OSCs employing nonfluorinated and fluorinated ZnPcs and CuPcs as donor, respectively. Details on the shown OSCs can be found in the Supporting Information.

are reanalyzed for this paper. The investigated devices comprise vacuum deposited small molecules in planar and bulk heterojunction architecture[12,37–39] and solution processed polymers.[8,11,40–42] We performed an intensive literature study to obtain the lowest energy $E_{T1}$ of either donor or acceptor, via one of the methods described above, see Table S1 in the Supporting Information for details.[40,43–58] We compare $E_{T1}$ to the $E_{CT}$ obtained from sensitive $EQE_{PV}$ spectra.[8,12] OSCs where $E_{T1} < E_{CT}$ are represented by blue dots. Devices where $E_{T1} > E_{CT}$ are shown by red dots. As outlined above, the determination of $E_{T1}$ has a significant uncertainty and, therefore, all OSCs where we find $E_{T1} - E_{CT} \leq \pm 100$ meV are represented by the grey dots.

In contrast to fluorescent OLED materials, where $T_1$ drives nonradiative recombination,[19,20] we find that in general, low energy $T_1$ states do not necessarily affect $\Delta V_{nr}$ in OSCs. The summarizing Figure 3 shows several devices around $E_{CT}$ = 1.5 eV which have similarly low $\Delta V_{nr}$ independently whether $E_{T1}$ is above or below $E_{CT}$. Furthermore, for devices with the highest $\Delta V_{nr}$, $T_1$ is actually higher in energy than $E_{CT}$. As previously reported, $\Delta V_{nr}$ depends on the absolute value of $E_{CT}$, rather than on the $E_{T1} - E_{CT}$ difference. The exception to this finding is the CuPc and fluorinated CuPc samples, discussed above, which are indicated with black diamonds in Figure 3.

In conclusion, we find that only in the cases with enhanced coupling to the ground state, $T_1$ limits the $V_{OC}$ and drives most of the recombination. However, in the most common cases, using small organic molecules or polymers, we find that the energetic position of $E_{T1}$ as compared to $E_{CT}$ is of secondary importance in determining $\Delta V_{nr}$ and the overall $V_{OC}$ losses of OSCs. Studies aiming at understanding and reducing $\Delta V_{nr}$ should instead focus on nonradiative CT state decay, even in the high voltage, low energy loss case where local triplet states are the lowest energy excited states.

## Experimental Section

*Device Preparation*: The layers of the OSCs of the metal–phthalocyanine series were thermally evaporated at ultrahigh vacuum (base pressure < $10^{-7}$ mbar) on a glass substrate with a prestructured indium tin oxide (ITO) contact (Thin Film Devices, USA). For an appropriate electron contact 15 nm of n-$C_{60}$, doped with $Cr_2(hpp)_4$ (Novaled GmbH, Germany) at 3 wt%, were deposited and followed by the active layer comprising 30 nm of donor molecule (zinc-phthalocyanine (ZnPc), CreaPhys GmbH, Germany) or copper-phthalocyanine (CuPc, abcr GmbH, Germany) or tetrafluoro-zinc-phthalocyanine ($F_4$ZnPc, BASF, Germany) or tetrafluoro-copper-phthalocyanine ($F_4$CuPc, synthesized by Dr. M. Lau) or tetrafluoro-zinc-phthalocyanine ($ZnF_4Pc$ or synthesized by Dr. B. Beyer) or tetrafluoro-copper-phthalocyanine ($CuF_4Pc$, synthesized by Dr. B. Beyer) coevaporated with $C_{60}$ (CreaPhys GmbH, Germany) at a 1:1 weight ratio. Afterward, 5 nm of an intrinsic hole transport layer (HTL) (*N,N′*-diphenyl-*N,N′*-bis(9,9-dimethyl-fluoren-2-yl)-benzidine (BF-DPB), Synthon Chemicals GmbH, Germany) or BPAPF (9,9-bis[4-(*N,N*-bis-biphenyl-4-yl-amino)phenyl]-9*H*-fluorene, Lumtec, Taiwan) and 40 nm of p-doped HTL (BF-DPB with 10 wt% NPD9 and BPAPF with 5 wt% NDP9; NDP9 is a p-dopant supplied by Novaled GmbH, Germany). The OSC was finished with 100 nm of Al. All the organic materials were purified 2–3 times by sublimation. The device was defined by the geometrical overlap of the bottom and the top contact and equaled 6.44 $mm^2$. To avoid exposure to ambient conditions, the organic part of the device was covered by a small glass substrate which was glued on top.

Current–voltage characteristics were measured with an SMU (Keithley 2400, USA) at standard testing conditions (16 S-150 V.3 Solar Light Co., USA) with a mismatch (mismatch = 0.62–0.76) corrected light intensity.

*Temperature Dependent Current–Voltage Measurements*: For temperature variation, the sample was mounted onto a temperature controlled copper block in vacuum, differences due to a temperature gradient in the substrate between temperature sensor (Type K thermocouple) and the active sample area were corrected by prior calibration. The systematic error for the temperature was estimated to be smaller than 5 K. The sample was illuminated by a white light LED. The $V_{OC}$ was measured with a source measure unit. It was interpolated from the two points of the current–voltage characteristic where the sign of the current density changed.

*Sensitive $EQE_{PV}$ Measurements*: The light of a quartz halogen lamp (50 W) was chopped at 140 Hz and coupled into a monochromator (Newport Cornerstone 260 1/4m, USA). The resulting monochromatic light was focused onto the OSC, its current at short-circuit conditions was fed to a current preamplifier before it was analyzed with a lock-in amplifier (Signal Recovery 7280 DSP, USA). The time constant of the lock-in amplifier was chosen to be 1 s and the amplification of the preamplifier was increased to resolve low photocurrents. The $EQE_{PV}$ was determined by dividing the photocurrent of the OSC by the flux of incoming photons, which was obtained with calibrated silicon (Si) and indium–gallium–arsenide (InGaAs) photodiode.

*Electroluminescence measurements* were obtained with an Andor SR393i-B spectrometer equipped with a cooled Si and cooled InGaAs detector array (DU420A-BR-DD and DU491A-1.7, UK). The spectral response of the setup was calibrated with a reference lamp (Oriel 63355). The emission spectrum of the OSCs was recorded at different injection currents, which correspond to applied voltages lower than or at least similar to the $V_{OC}$ of the device at 1 sun illumination.

*Computational Details*: The ground-state geometric structure of the donor compounds was optimized at the density functional theory level with the calculation's suite Gaussian 16.[59] The HSE06 exchange–correlation functional was used,[60] as in a previous work.[61] The 6-31G(d,p) basis set was employed for nonmetallic atoms, while a larger one was chosen for Cu and Zn, namely AUG-cc-pVTZ. The $D_{4h}$ symmetry point group was imposed throughout the geometry optimization process. Then, CASSCF calculations were carried out on the optimized structures with the ORCA 4.0.1 suite.[62] A Def2-TZVPP basis set was used, along with the RIJCOSX approximation to speed up the calculations. An n-electron valence state perturbation theory (NEVPT2) approach, as implemented in the ORCA code, was introduced in order to correct the CASSCF energies for dynamic correlation effects. At last, spin–orbit coupling relativistic effects were added to refine the NEVPT2 transition energies and assess the associated oscillator strengths.

## Supporting Information

Supporting Information is available from the Wiley Online Library or from the author.

## Acknowledgements

This work was supported by the German Federal Ministry for Education and Research (BMBF) through the InnoProfile project "Organische p-i-n Bauelemente 2.2" and the European Union's Horizon 2020 research and innovation programme under Marie Sklodowska Curie Grant agreement No.722651 (SEPOMO). F.P. and D.N. acknowledge funding by the German Research Foundation (DFG) via the SFB 951 "HIOS". The authors acknowledge Prof. K. Leo and V. C. Nikolis for fruitful discussions. The authors thank Dr. B. Beyer for supplying $ZnF_4Pc$ and $CuF_4Pc$ as well as Dr. M. Lau for the synthesis of $F_4$CuPc. Additionally, the authors thank Prof. Bäuerle from University of Ulm for the supply of DH4T, DH6T, and several $DCV_2$-nT-R. Furthermore, the authors

acknowledge Dr. F. Holzmueller, M. Saalfrank, and Dr. R. Meerheim for providing OSC devices for this study. Computational resources were provided by the Consortium des Équipements de Calcul Intensif (CÉCI), funded by the Fonds de la Recherche Scientifiques de Belgique (F.R.S.-FNRS) under Grant No. 2.5020.11, as well as the Tier-1 supercomputer of the Fédération Wallonie-Bruxelles, infrastructure funded by the Walloon Region under Grant Agreement No. 1117545. D.B. is a FNRS Research Director.

## Conflict of Interest

The authors declare no conflict of interest.

## Keywords

charge-transfer states, nonradiative voltage losses, organic solar cells, triplet excited states

Received: February 8, 2018
Revised: March 9, 2018
Published online:

[1] K. Leo, *Nat. Rev. Mater.* **2016**, *1*, 16056.
[2] J. E. Carlé, F. C. Krebs, *Sol. Energy Mater. Sol. Cells* **2013**, *119*, 309.
[3] S. B. Darling, F. You, *RSC Adv.* **2013**, *3*, 17633.
[4] K. Leo, *Nat. Nanotechnol.* **2015**, *10*, 574.
[5] M. A. Green, K. Emery, Y. Hishikawa, W. Warta, E. D. Dunlop, D. H. Levi, A. W. Y. Ho-Baillie, *Prog. Photovoltaics* **2017**, *25*, 659.
[6] V. C. Nikolis, J. Benduhn, F. Holzmueller, F. Piersimoni, M. Lau, O. Zeika, D. Neher, C. Koerner, D. Spoltore, K. Vandewal, *Adv. Energy Mater.* **2017**, *7*, 1700855.
[7] U. Rau, *Phys. Rev. B* **2007**, *76*, 085303.
[8] K. Vandewal, K. Tvingstedt, A. Gadisa, O. Inganäs, J. V. Manca, *Phys. Rev. B* **2010**, *81*, 125204.
[9] W. Shockley, H. J. Queisser, *J. Appl. Phys.* **1961**, *32*, 510.
[10] H. J. Queisser, *Mater. Sci. Eng. B* **2009**, *159–160*, 322.
[11] K. Vandewal, K. Tvingstedt, A. Gadisa, O. Inganäs, J. V. Manca, *Nat. Mater.* **2009**, *8*, 904.
[12] J. Benduhn, K. Tvingstedt, F. Piersimoni, S. Ullbrich, Y. Fan, M. Tropiano, K. A. McGarry, O. Zeika, M. K. Riede, C. J. Douglas, S. Barlow, S. R. Marder, D. Neher, D. Spoltore, K. Vandewal, *Nat. Energy* **2017**, *2*, 17053.
[13] K. Vandewal, Z. F. Ma, J. Bergqvist, Z. Tang, E. G. Wang, P. Henriksson, K. Tvingstedt, M. R. Andersson, F. L. Zhang, O. Inganäs, *Adv. Funct. Mater.* **2012**, *22*, 3480.
[14] J. Yao, T. Kirchartz, M. S. Vezie, M. a. Faist, W. Gong, Z. He, H. Wu, J. Troughton, T. Watson, D. Bryant, J. Nelson, *Phys. Rev. Appl.* **2015**, *4*, 014020.
[15] M. A. Green, *Prog. Photovoltaics* **2012**, *20*, 472.
[16] K. Tvingstedt, O. Malinkiewicz, A. Baumann, C. Deibel, H. J. Snaith, V. Dyakonov, H. J. Bolink, *Sci. Rep.* **2014**, *4*, 06071.
[17] W. Tress, *Adv. Energy Mater.* **2017**, *7*, 1602358.
[18] N. A. Ran, J. A. Love, C. J. Takacs, A. Sadhanala, J. K. Beavers, S. D. Collins, Y. Huang, M. Wang, R. H. Friend, G. C. Bazan, T. Q. Nguyen, *Adv. Mater.* **2016**, *28*, 1482.
[19] A. Köhler, H. Bässler, *Mater. Sci. Eng., R* **2009**, *66*, 71.
[20] A. Rao, P. C. Y. Chow, S. Gelinas, C. W. Schlenker, C.-Z. Li, H.-L. Yip, A. K.-Y. Jen, D. S. Ginger, R. H. Friend, *Nature* **2013**, *500*, 12339.
[21] F. Etzold, I. A. Howard, N. Forler, A. Melnyk, D. Andrienko, M. R. Hansen, F. Laquai, *Energy Environ. Sci.* **2015**, *8*, 1511.
[22] D. W. Gehrig, I. A. Howard, F. Laquai, *J. Phys. Chem. C* **2015**, *119*, 13509.
[23] P. C. Y. Chow, S. Gélinas, A. Rao, R. H. Friend, S. Gélinas, A. Rao, R. H. Friend, *J. Am. Chem. Soc.* **2014**, *136*, 3424.
[24] M. G. Cory, M. C. Zerner, *Chem. Rev.* **1991**, *91*, 813.
[25] I. Bruder, J. Schöneboom, R. Dinnebier, A. Ojala, S. Schäfer, R. Sens, P. Erk, J. Weis, *Org. Electron.* **2010**, *11*, 377.
[26] F. Piersimoni, D. Cheyns, K. Vandewal, J. V. Manca, B. P. Rand, *J. Phys. Chem. Lett.* **2012**, *3*, 2064.
[27] P. S. Vincett, E. M. Voigt, K. E. Rieckhoff, *J. Chem. Phys.* **1971**, *55*, 4131.
[28] W. Y. Tong, H. Y. Chen, A. B. Djurišić, A. M. Ng, H. Wang, S. Gwo, W. K. Chan, *Opt. Mater.* **2010**, *32*, 924.
[29] A. G. Kazanski, E. I. Terukov, A. V. Ziminov, O. B. Gusev, A. V. Fenukhin, A. G. Kolosko, I. N. Trapeznikova, Y. A. Nikolaev, B. Modu, *Tech. Phys. Lett.* **2005**, *31*, 782.
[30] A. V. Fenukhin, A. G. Kazanskii, A. G. Kolosko, E. I. Terukov, A. V. Ziminov, *J. Non-Cryst. Solids* **2006**, *352*, 1668.
[31] T. Mayer, U. Weiler, C. Kelting, D. Schlettwein, S. Makarov, D. Wöhrle, O. Abdallah, M. Kunst, W. Jaegermann, *Sol. Energy Mater. Sol. Cells* **2007**, *91*, 1873.
[32] T. M. Burke, S. Sweetnam, K. Vandewal, M. D. McGehee, *Adv. Energy Mater.* **2015**, *5*, 1500123.
[33] H. Uoyama, K. Goushi, K. Shizu, H. Nomura, C. Adachi, *Nature* **2012**, *492*, 234.
[34] A. Köhler, J. S. Wilson, R. H. Friend, M. K. Al-Suti, M. S. Khan, A. Gerhard, H. Bässler, *J. Chem. Phys.* **2002**, *116*, 9457.
[35] A. Köhler, D. Beljonne, *Adv. Funct. Mater.* **2004**, *14*, 11.
[36] A. P. Monkman, H. D. d. G. M. M. Burrows, I. Hamblett, S. Navaratnam, *Chem. Phys. Lett.* **1999**, *307*, 303.
[37] T. Moench, P. Friederich, F. Holzmueller, B. Rutkowski, J. Benduhn, T. Strunk, C. Koerner, K. Vandewal, A. Czyrska-Filemonowicz, W. Wenzel, K. Leo, *Adv. Energy Mater.* **2016**, *6*, 1501280.
[38] R. Fitzner, E. Mena-Osteritz, A. Mishra, G. Schulz, E. Reinold, M. Weil, C. Koerner, H. Ziehlke, C. Elschner, K. Leo, M. Riede, M. Pfeiffer, C. Uhrich, P. Bäuerle, *J. Am. Chem. Soc.* **2012**, *134*, 11064.
[39] C. Koerner, C. Elschner, N. C. Miller, R. Fitzner, F. Selzer, E. Reinold, P. Bäuerle, M. F. Toney, M. D. McGehee, K. Leo, M. Riede, *Org. Electron.* **2012**, *13*, 623.
[40] E. T. Hoke, K. Vandewal, J. A. Bartelt, W. R. Mateker, J. D. Douglas, R. Noriega, K. R. Graham, J. M. J. Fréchet, A. Salleo, M. D. Mcgehee, *Adv. Energy Mater.* **2013**, *3*, 220.
[41] K. Vandewal, A. Gadisa, W. D. Oosterbaan, S. Bertho, F. Banishoeib, I. Van Severen, L. Lutsen, T. J. Cleij, D. Vanderzande, J. V. Manca, *Adv. Funct. Mater.* **2008**, *18*, 2064.
[42] K. Vandewal, W. D. Oosterbaan, S. Bertho, V. Vrindts, A. Gadisa, L. Lutsen, D. Vanderzande, J. V. Manca, *Appl. Phys. Lett* **2009**, *95*, 21.
[43] J. W. Arbogast, A. P. Darmanyan, C. S. Foote, Y. Rubin, F. N. Diederich, M. M. Alvarez, S. J. Anz, R. L. Whetten, *J. Phys. Chem.* **1991**, *95*, 11.
[44] D. Beljonne, J. Cornil, R. H. Friend, R. A. J. Janssen, J. L. Brédas, *J. Am. Chem. Soc.* **1996**, *118*, 6453.
[45] D. Di Nuzzo, A. Aguirre, M. Shahid, V. S. Gevaerts, S. C. J. Meskers, R. A. J. Janssen, *Adv. Mater.* **2010**, *22*, 4321.
[46] K. Goushi, K. Yoshida, K. Sato, C. Adachi, *Nat. Photonics* **2012**, *6*, 253.
[47] R. R. Hung, J. J. Grabowski, *J. Phys. Chem.* **1991**, *95*, 6073.
[48] D. K. K. Liu, L. R. Faulkner, *J. Am. Chem. Soc.* **1977**, *99*, 4594.
[49] K. Sato, K. Shizu, K. Yoshimura, A. Kawada, H. Miyazaki, C. Adachi, *Phys. Rev. Lett.* **2013**, *110*, 247401.
[50] R. Schueppel, K. Schmidt, C. Uhrich, K. Schulze, D. Wynands, J. L. Brédas, E. Brier, E. Reinold, H.-B. Bu, P. Baeuerle, B. Maennig, M. Pfeiffer, K. Leo, *Phys. Rev. B* **2008**, *77*, 85311.

 

[51] J. S. Swensen, E. Polikarpov, A. Von Ruden, L. Wang, L. S. Sapochak, A. B. Padmaperuma, *Adv. Funct. Mater.* **2011**, *21*, 3250.
[52] D. Veldman, S. C. J. Meskers, R. A. J. Janssen, *Adv. Funct. Mater.* **2009**, *19*, 1939.
[53] M. R. Wasielewski, M. P. O'Neil, K. R. Lykke, M. J. Pellin, D. M. Gruen, *J. Am. Chem. Soc.* **1991**, *113*, 2774.
[54] R. M. Williams, J. M. Zwier, J. W. Verhoeven, *J. Am. Chem. Soc.* **1995**, *117*, 4093.
[55] B. Xu, S. Holdcroft, *Adv. Mater.* **1994**, *6*, 325.
[56] C. Murawski, C. Fuchs, S. Hofmann, K. Leo, M. C. Gather, *Appl. Phys. Lett.* **2014**, *105*, 113303.
[57] I. Lim, E.-K. Kim, S. A. Patil, D. Y. Ahn, W. Lee, N. K. Shrestha, J. K. Lee, W. K. Seok, C.-G. Cho, S.-H. Han, *RSC Adv.* **2015**, *5*, 55321.
[58] S. Pfuetzner, A. Petrich, C. Malbrich, J. Meiss, M. Koch, M. K. Riede, M. Pfeiffer, K. Leo, *Proc. SPIE 6999 Organic Optoelectronics and Photonics III*, SPIE Photonics Europe, Strasbourg, France **2008**, https://doi.org/10.1117/12.782412 (accessed: April 2008).
[59] M. J. Frisch, G. W. Trucks, H. B. Schlegel, G. E. Scuseria, M. A. Robb, J. R. Cheeseman, G. Scalmani, V. Barone, G. A. Petersson, H. Nakatsuji, X. Li, M. Caricato, A. V. Marenich, J. Bloino, B. G. Janesko, R. Gomperts, B. Mennucci, H. P. Hratchian, J. V. Ortiz, A. F. Izmaylov, J. L. Sonnenberg, D. Williams-Young, F. Ding, F. Lipparini, F. Egidi, J. Goings, B. Peng, A. Petrone, T. Henderson, D. Ranasinghe, V. G. Zakrzewski, J. Gao, N. Rega, G. Zheng, W. Liang, M. Hada, M. Ehara, K. Toyota, R. Fukuda, J. Hasegawa, M. Ishida, T. Nakajima, Y. Honda, O. Kitao, H. Nakai, T. Vreven, K. Throssell, J. J. A. Montgomery, J. E. Peralta, F. Ogliaro, M. J. Bearpark, J. J. Heyd, E. N. Brothers, K. N. Kudin, V. N. Staroverov, T. A. Keith, R. Kobayashi, J. Normand, K. Raghavachari, A. P. Rendell, J. C. Burant, S. S. Iyengar, J. Tomasi, M. Cossi, J. M. Millam, M. Klene, C. Adamo, R. Cammi, J. W. Ochterski, R. L. Martin, K. Morokuma, O. Farkas, J. B. Foresman, D. J. Fox, Gaussian 16 Revision A.03, Gaussian Inc., Wallingford, CT **2016**.
[60] J. Heyd, G. E. Scuseria, *J. Chem. Phys.* **2004**, *121*, 1187.
[61] N. Marom, O. Hod, G. E. Scuseria, L. Kronik, *J. Chem. Phys.* **2008**, *128*, 164107.
[62] F. Neese, *WIREs Comput. Mol. Sc.* **2012**, *2*, 73.